JOURNAL OF MATERIALS SCIENCE **37** (2002) 3953 – 3958

Properties of GaAs nanoclusters deposited by a femtosecond laser

L. N. DINH, S. E. HAYES, A. E. WYNNE, M. A. WALL, C. K. SAW, B. C. STUART, M. BALOOCH
Lawrence Livermore National Laboratory, Livermore, CA 94551, USA

A. K. PARAVASTU, J. A. REIMER
University of California, Berkeley, CA 94720, USA

The properties of femtosecond pulsed laser deposited GaAs nanoclusters were investigated. Nanoclusters of GaAs were produced by laser ablating a single crystal GaAs target in vacuum or Ar gas. Atomic force and transmission electron microscopies showed that most of the clusters were spherical and ranged in diameter from 1 nm to 50 nm, with a peak size distribution between 5 nm and 9 nm, depending on the Ar gas pressure or laser fluence. X-ray diffraction, solid-state nuclear magnetic resonance, Auger electron spectroscopy, electron energy loss spectroscopy, and high-resolution transmission electron microscopy revealed that these nanoclusters were randomly oriented GaAs crystallites. An oxide outer shell of ∼2 nm developed subsequently on the surfaces of the nanocrystals as a result of transportation in air. Unpassivated GaAs nanoclusters exhibited no detectable photoluminescence. After surface passivation, these nanoclusters displayed photoluminescence energies less than that of bulk GaAs from which they were made. Our photoluminescence experiments suggest an abundance of sub-band gap surface states in these GaAs nanocrystals.

1. Introduction

GaAs nanocrystals are expected to exhibit novel size dependent properties due to quantum confinement effects, such as the quantization of the electronic density of states, and the blue shift of the optical absorption and photoluminescence with smaller crystal sizes [1, 2]. Among the techniques employed in the production of GaAs, pulsed laser deposition (PLD) seems to be a suitable choice for the deposition of thin GaAs films or nanoclusters on different substrates. The main advantages of PLD are its simple experimental setup and the ability to operate in a wide range of gas pressures. For complex materials with constituent elements having greatly different vapor pressures, laser ablation with short pulsed lasers has produced films with excellent stoichiometries [3]. There have been published studies concerning the formation of GaAs nanostructures by laser ablation with nanosecond lasers, the evolution of the GaAs target under ultrashort pulsed lasers, the properties of the ablated plumes, and the generation of two and three dimensionally confined structures of GaAs by techniques other than PLD [4–17]. However, to our knowledge, there is no published report on GaAs nanoclusters formed by femtosecond lasers. In this paper, we described the characteristics of GaAs nanoclusters synthesized via femtosecond laser deposition.

2. Experiments

The output at 810 nm of a 150 femtosecond Ti-Sapphire laser operating at 1000 Hz, was employed in the growth of GaAs nanoclusters [18]. With a time averaged power of 2 W and a circular spot diameter of 0.85 mm at the ablation target, the laser beam had an average energy density of 0.35 J/cm^2 per pulse. Samples were synthesized in a high vacuum chamber with a base pressure of about 1.3×10^{-3} Pa. For the production of GaAs nanoclusters, the chamber gate valve connected to the pumping system was closed, and Ar gas was leaked into the chamber up to the desired pressure. During the ablation process, a p-type (100) GaAs single crystal wafer with a diameter of 5.08 cm was rotated while the laser beam was translated over the surface so that the whole wafer surface was utilized in a fairly uniform manner [19]. GaAs nanoclusters were deposited onto glass slides, metal foils, Si wafers, and highly oriented pyrolytic graphite (HOPG) substrates; all were at room temperature and mounted on a holder located about 15 cm away and parallel to the GaAs target. After deposition, the samples were removed from the synthesis chamber and transported in air to the appropriate analysis stations for x-ray diffraction (XRD), atomic force microscopy (AFM), scanning electron microscopy (SEM), Auger electron spectroscopy (AES), transmission electron microscopy (TEM), electron energy loss spectroscopy (EELS), photoluminescence (PL) spectroscopy, and solid-state nuclear magnetic resonance (NMR).

3. Results

Fig. 1 shows AFM images of less than one layer (a) and many layers (b) of nanoclusters deposited in a vacuum

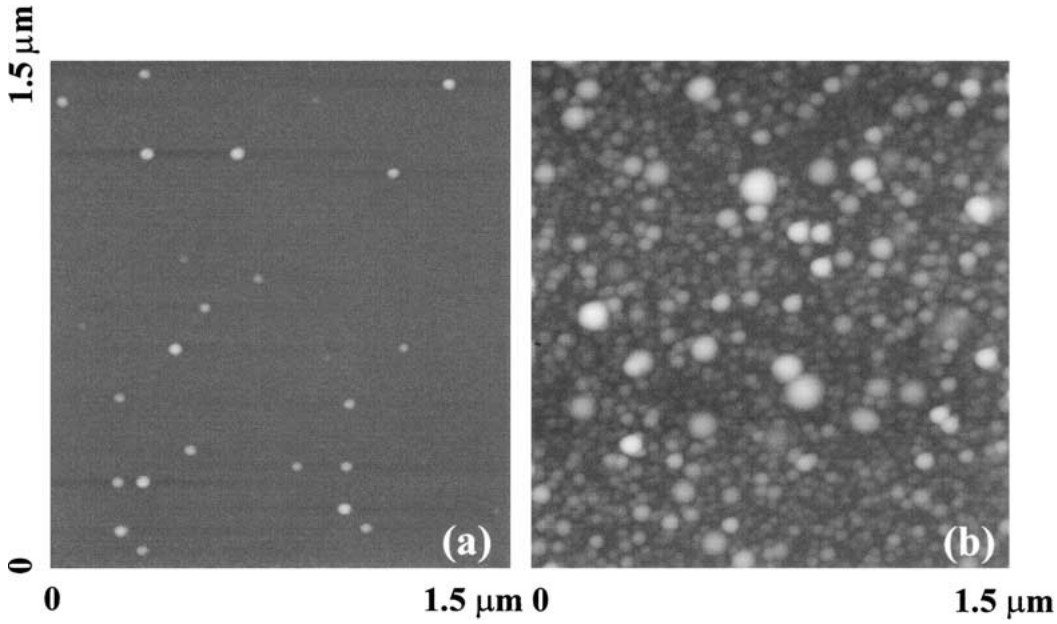

Figure 1 AFM images of less than one layer (a) and many layers (b) of nanoclusters deposited in a high vacuum of 1.3×10^{-3} Pa onto Si(100) substrates.

of 1.3×10^{-3} Pa onto Si(100) substrates. Clusters with sizes ranging from 1 nm to 50 nm were measured for these samples. Due to the convolution of the clusters' dimensions with the finite radius of the tip, AFM diameter measurements tend to give values that are artificially high and so may create a false impression that measured nanoclusters have a flattened pancake shape. The apparent width, w, of a spherical object of height h due to the convolution with an AFM spherical tip of diameter d is given by $d = w^2/4h$ [20]. So spherical objects with diameters in the range of 1 nm to 50 nm have images with an apparent widths from 20 nm to 141 nm if the tip radius is 50 nm. Upon deconvolution, the nanoclusters reported in this paper have lateral dimensions comparable to height measurements, suggesting a fairly spherical shape for the nanoclusters.

The deposition rate for the nanocluster film shown in Fig. 1b on a 5.08 cm wafer substrate located 15 cm away and parallel to the GaAs target was on the order of 0.15 nm/s, and the nanocluster film distribution could be fitted to a cosine to the power of 6.7 ± 1.7 about the ablated spot in vacuum. This angular distribution is comparable to cosine to the power of 5–8 associated with laser ablation of many different materials by nanosecond lasers [3, 21, 22].

Fig. 2 shows the size distribution of the nanoclusters as a function of Ar pressure from 1.3×10^{-3} to 3188 Pa at a laser fluence of 0.35 J/cm^2. Most of the clusters had sizes ranging from 2 nm to 20 nm, with a modest upward shift of the dominant peak size from 5.5 nm to 7.5 nm as the Ar pressure increased. This trend is opposite to that observed in nanoclusters of materials with higher melting temperatures such as ZnO and Y_2O_3 nanoclusters [21, 22]. An increase in the average particle size with increasing Ar pressure suggests that very small clusters, molecules and/or monomers collide in the plume, leading to a larger average nanocrystal size and thus a significant dependence on pressure such as found when laser ablating ZnO or Y_2O_3 [21, 22]. The fact that GaAs nanocluster sizes did not increase appreciably with increasing Ar pressure suggests that only a small fraction of ejected materials was in the form of molecules or monomers. It is likely that the formation of the nanoclusters described in the present paper occurs predominantly near the surface of the ablated GaAs target in the form of nanodropplets due to hydrodynamic sputtering. And assumed that most of the ejected materials are GaAs nanodropplets, which are much more heavier than the Ar atoms in the background, collisions with Ar gas will not effectively help the nanodropplets to deflect and grow by coagulation.

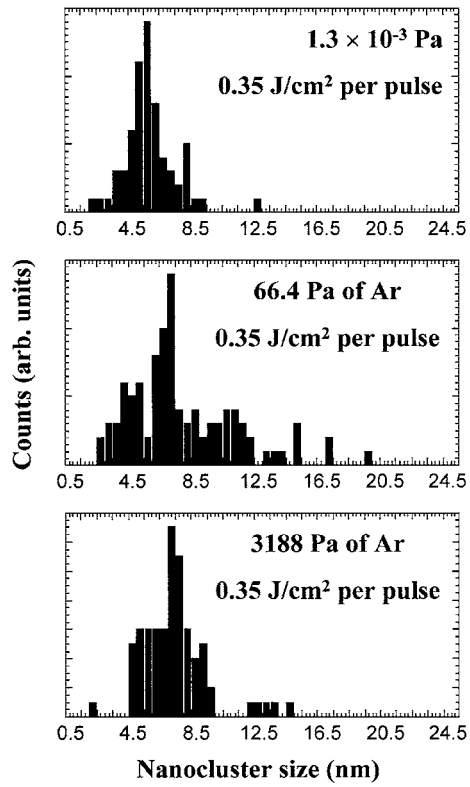

Figure 2 The size distribution of the nanoclusters as a function of Ar background pressure.

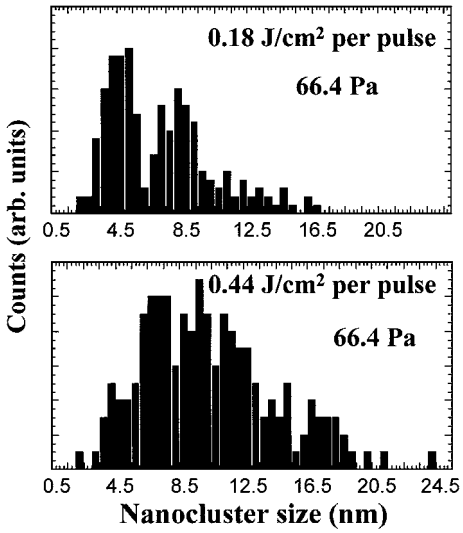

Figure 3 The size distribution of the nanoclusters collected at the substrates at an Ar pressure of 66.4 Pa as a function of laser fluence.

One difference between nanocluster films synthesized at 1.3×10^{-3} and those synthesized in Ar is in the film morphology: in vacuum, the clusters tended to form a continuous solid film, whereas a powder-like film resulted when Ar was present. This is because in an Ar background, the laser ablated nanoclusters experienced numerous collisions with the Ar atoms during the flight path from the target to the substrate, causing them to lose much of their kinetic energies prior to impacting the substrate. At an Ar pressure of ∼0.1 Pa, the nanoclusters collected on different substrates already had the look of, and behaved mechanically like, powders. Fig. 3 shows the size distribution of the nanoclusters collected at the substrates in an Ar pressure of 66.4 Pa as a function of laser fluence from 0.18 J/cm^2 to 0.44 J/cm^2. Most of the clusters have diameters ranging from 2 nm to 20 nm, with a modest upward shift of the dominant peak size from ∼5 nm to ∼9 nm as the laser fluence increased from 0.18 to 0.44 J/cm^2. Within experimental errors and limited statistics, we conclude that the sizes of the nanoclusters did not appreciably vary with laser fluence from 0.18 J/cm^2 per pulse to 0.44 J/cm^2 per pulse.

Fig. 4 shows the XRD spectrum of a nanocluster film that was several microns thick. It is seen from this

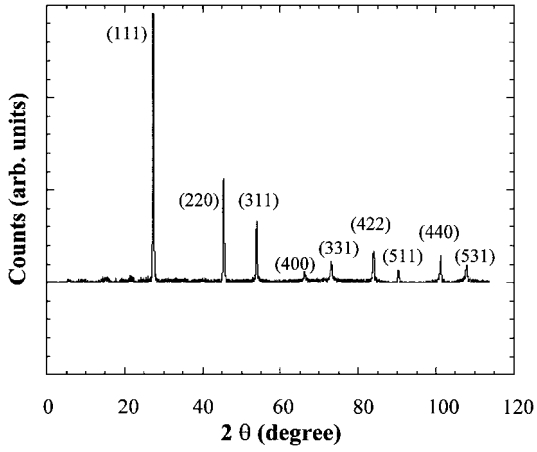

Figure 4 The XRD spectrum of a nanocluster film several micrometers thick, revealing the randomly oriented crystalline nature of the nanoclusters.

spectrum that the film was composed mostly of randomly oriented GaAs crystallites. Fig. 5 shows a low resolution TEM image of GaAs nanoclusters synthesized in 132 Pa of Ar. The GaAs nanoclusters were transferred onto an amorphous carbon coated TEM grid after the vacuum synthesis by touching the TEM grid on a substrate surface heavily coated with GaAs nanocluster powders. The nanocluster density appears rather high, with most individual nanoclusters sticking to one another due to electrostatic and van der Waals forces. However, where the nanocluster density is thinner, one can observe and measure the diameters of individual nanoclusters. The spherical shape of the nanoclusters is experimentally confirmed here since AFM height measurements agree well with TEM lateral measurements. Fig. 6 shows a TEM image of nanoclusters on an amorphous carbon coated TEM grid (a) and the corresponding gallium (b), arsenic (c), and oxygen (d) maps obtained using EELS. The dark regions in Fig. 6a represent areas with nanoclusters, as in Fig. 5, while dark areas in Fig. 6b–d represent areas void of the element being mapped. It is clear from Fig. 6 that wherever there are clusters, there are gallium, arsenic, and oxygen signals. Fig. 7 shows a high resolution TEM image of a synthesized nanocluster. It is seen that this nanocluster is composed of a crystalline core of ∼6 nm and an amorphous outer layer of ∼2 nm. The distance between lattice fringes in Fig. 7 is about 0.33 nm and corresponds to a diffractive interference pattern from GaAs (111) planes. We conclude that the basic structure of the nanoclusters formed by femtosecond laser ablation of a GaAs (100) target is nanocrystalline GaAs. An oxide outer shell developed subsequently during transportation, in air, of the nanoclusters from the synthesis chamber to the analysis chambers. In a previous publication, we reported the formation of GaAs nanoclusters by a 50 nanosecond Cu-vapor laser [10]. There, the outer shells of the GaAs nanoclusters were noted to be composed of both arsenic oxide and gallium oxide following air exposure [10]. Note that exposure of GaAs to oxygen, moisture, or air creates an amorphous native oxide layer which is composed of gallium oxide and arsenic oxide and is a few nanometers in thickness [10, 23–25]. For the GaAs nanocrystals synthesized with the 50 nanosecond Cu-vapor laser, then exposed to air, the amorphous oxide was rich in arsenic oxide independent of the Ar pressure suggesting a sub-stoichiometry at or near the nanocrystal surfaces [10]. In this report, AES of the clusters formed by laser ablating a GaAs single crystal target in an Ar pressure of 132 Pa revealed the existence of gallium, arsenic, and oxygen with a Ga to As ratio of 1 to 1 in the outer shells suggesting a uniform stoichiometry for these nanoclusters. The implication of this is that if we can come up with a way to passivate the surface of these GaAs nanoclusters (against oxidation) right in the synthesis chamber before taking them out to ambient air, femtosecond laser ablation can deliver stoichiometric GaAs nanocrystals inside out.

Solid-state NMR spectra of the GaAs nanoclusters acquired via Bloch decay under static conditions (90° pulse of 5.5 μs, recycle delays of 2–3 s) confirmed that there is a single ^{71}Ga resonance at a chemical shift

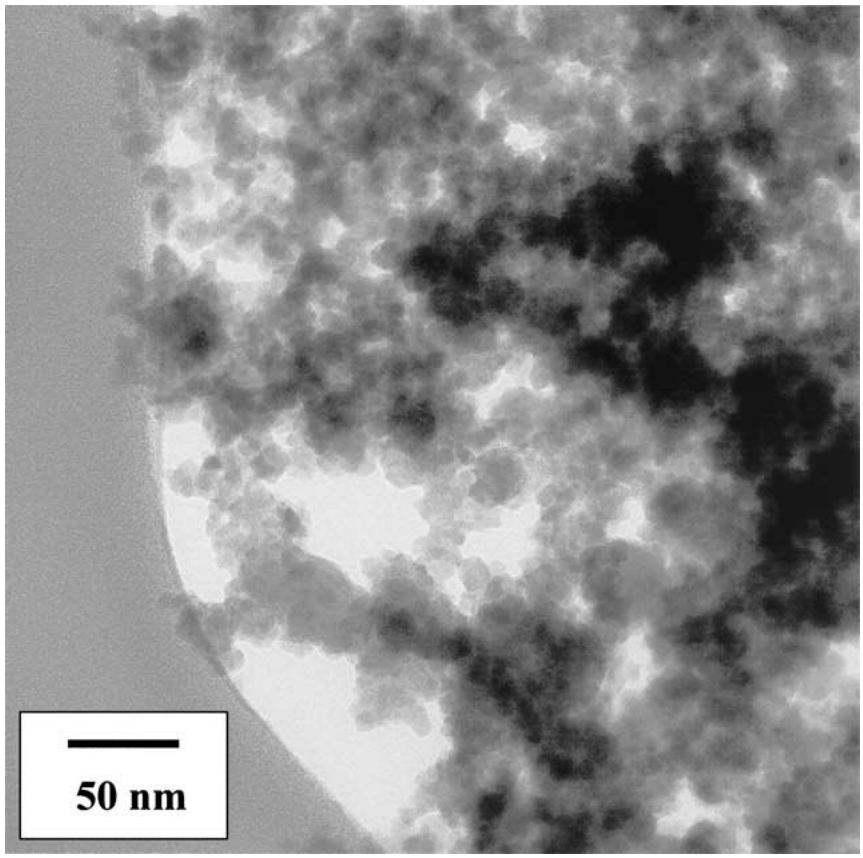

Figure 5 A low resolution TEM image of GaAs nanoclusters synthesized in 132 Pa of Ar. The GaAs nanoclusters were transferred onto an amorphous carbon coated TEM grid after the vacuum synthesis by touching the TEM grid on a substrate heavily coated with a powder film of GaAs nanocluster.

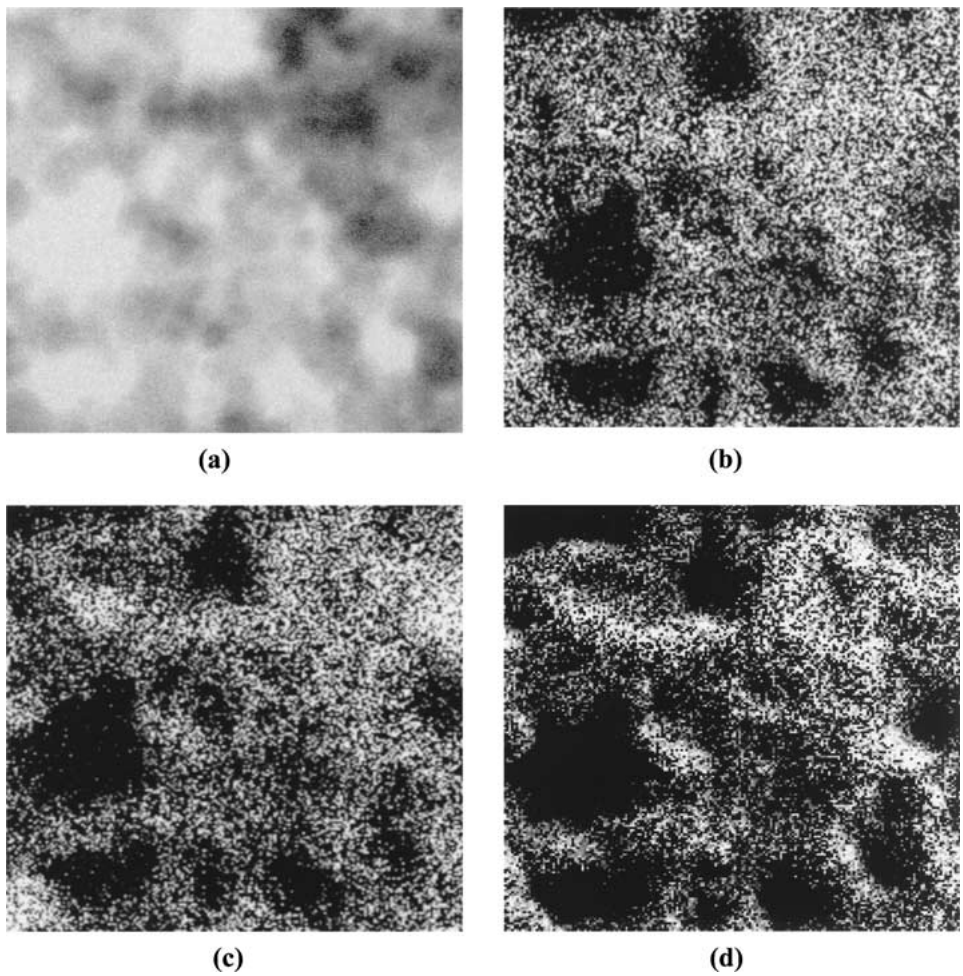

Figure 6 A TEM image of nanoclusters on an amorphous carbon coated TEM grid (a) and the corresponding Ga (b), As (c), and O (d) maps obtained using EELS.

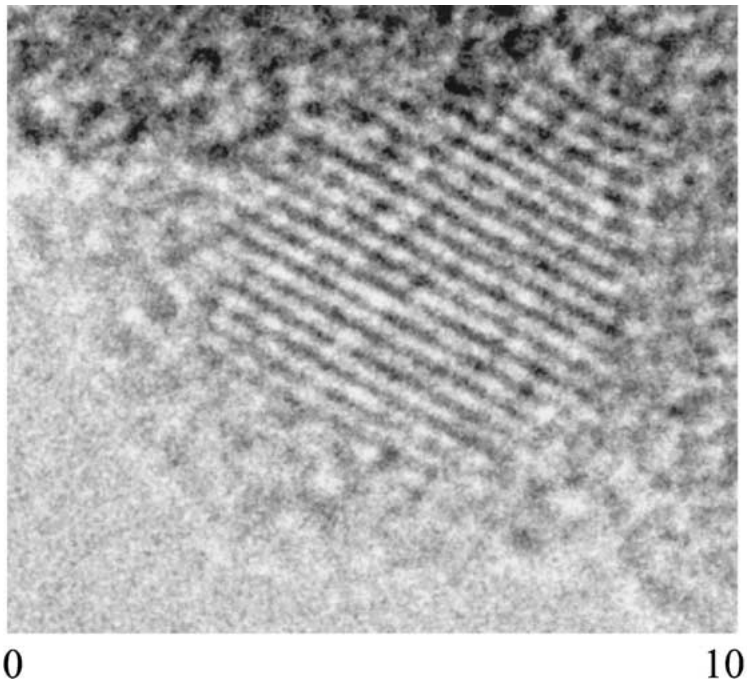

Figure 7 A high resolution TEM image of a nanocluster showing a GaAs crystalline core and an amorphous oxide outer shell.

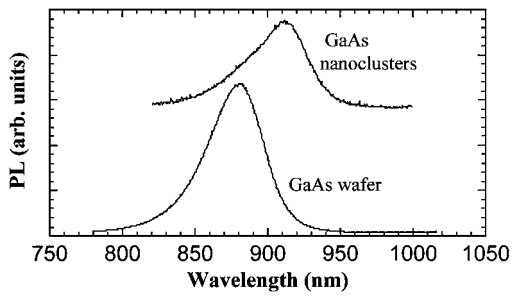

Figure 8 PL of the target and passivated GaAs nanocrystals. The red shift in PL from the GaAs nanoclusters is due to the existence of sub-band gap surface passivation states.

equivalent to that of bulk GaAs (224 ppm, fwhm = 3 kHz), indicative of ^{71}Ga with cubic site symmetry. We attribute this signal to the crystalline cores of the nanoclusters, theorizing that the amorphous outer shells will be significantly broadened and thus difficult to detect via NMR. Combining all the structural methods, we conclude that laser ablating a GaAs single crystal wafer with a femtosecond laser at 810 nm and with a laser fluence of 0.18–0.44 J/cm^2 per pulse yielded randomly oriented GaAs nanocrystals, the outer surface layers of which became oxidized upon air exposure.

Upon excitation by photon at 532 nm from a solid state laser [26], these nanocrystals showed no detectable PL. Since these nanocrystals have been exposed to air during transport to the PL station, they contained a 1–2 nm thick native oxide on the surface [10, 27]. Native oxide layers on semiconductors are known to be non-stoichiometric and full of sub-band gap surface states, thereby suppressing PL [27]. Upon etching the oxide layer away with a $H_2O : H_2O_2 : H_2SO_4$ (500 : 8 : 1) solution and passivating with a 1.0 M solution of Na_2S [28], the GaAs nanoclusters displayed PL that was red shifted by 30 nm compared with the PL from the bulk single crystal target (see Fig. 8). At the sizes reported here, GaAs quantum dots are expected to exhibit large blue shift in the band gaps due to the quantum confinement effects [29–31]. So, we tentatively attribute the red shift in PL from our GaAs nanoclusters to the existence of sub-band gap surface passivation states.

4. Summary

We have presented the synthesis and properties of GaAs nanoclusters deposited on substrates by laser ablating single crystal GaAs target with a femtosecond laser. Our results show that these nanoclusters were randomly oriented GaAs nanocrystals with the majority of the crystallites ranging in size from 2 nm to 20 nm. GaAs nanocrystals obtained with the femtosecond laser presented here are stoichiometric [10]. Increasing the laser fluence from 0.18 to 0.44 J/cm^2 or Ar pressure from 1.3×10^{-3} Pa to 3188 Pa shifted cluster peak size very little. We hypothesize that, above a minimum laser fluence threshold, the laser-target interaction forms GaAs nanodroplets very near the surface of the GaAs target due to hydrodynamic sputtering. Upon air exposure, the nanocrystals developed a native oxide layer of 1–2 nm on the surface. Removal of this oxide layer and surface passivation were required for detecting PL from the clusters; yet passivated clusters still red-shifted in comparison with the PL from the single crystal GaAs target. We suggest this is due to the surface states introduced by the passivation layer itself.

To our knowledge, this is the first ever report on the formation of stoichiometric GaAs nanocrystals by a femtosecond laser. Due to limitation in our current experimental setup, many scientific questions remain unsanswered in this report such as: the cause for the difference in the stoichiometries at the surfaces of the GaAs nanoclusters synthesized by the 50 nanosecond Cu-vapor laser and the femtosecond laser described in this paper; how stoichiometric GaAs nanocrystals are

formed by femtosecond laser ablation; if the size distribution measured on the surface is the same as that for clusters in the gas phase; how the clusters might migrate at room temperature to form larger particles; or what is the dependence of the properties of the clusters on the laser wavelength and etc. We are currently having plans to do plume analysis and *in situ* target characterization in addition to cluster measurement at the substrates to answer these questions. We will report these results when they are available in a future publication.

Acknowledgment

This work was performed under the auspices of the U.S. Department of Energy by the University of California Lawrence Livermore National Laboratory under contract No. W-7405-ENG-48.

References

1. C. WEISBUCH and B. VINTER, "Quantum Semiconductor Structures" (Academic Press, San Diego, CA, 1991).
2. U. WOGGON, "Optical Properties of Semiconductor Quantum Dots" (Springer-Verlag, Berlin, 1997).
3. D. B. CHRISEY and G. K. HUBLER, "Pulsed Laser Deposition of Thin Films" (John Wiley & Sons, New York, 1994).
4. M. OKIGAWA, T. NAKAYAMA, K. TAKAYAMA and N. ITOH, *Solid State Commun*. **49** (1984) 347.
5. K. ICHIGE, Y. MATSUMOTO and A. NAMIKI, *Nucl. Instrum. Methods* B **33** (1988) 820.
6. C. GARCIA, J. RAMOS, A. C. PRIETO, J. JIMENEZ, C. GEERTSEN, J. L. LACOUR and P. MAUCHIEN, *Appl. Surf. Sci.* **96–98** (1996) 370.
7. V. CRACIUN and D. CRACIUN, *ibid*. **109/110** (1997) 312.
8. A. OKANO, J. KANASAKI, Y. NAKAI and N. ITOH, *J. Phys.: Condens. Matter*. **6** (1994) 2697.
9. L. WANG, K. W. D. LEDINGHAM, C. J. MCLEAN and R. P. SINGHAL, *Appl. Phys*. B **54** (1992) 71.
10. L. N. DINH, S. HAYES, C. K. SAW, W. MCLEAN II, M. BALOOCH and J. A. REIMER, *APL* **75** (1999) 2208.
11. V. I. SRDANOV, I. ALXNEIT, G. D. STUCKY, C. M. REAVES and S. P. DENBAARS, *J. Phys. Chem*. B **102** (1998) 3341.
12. D. I. LUBYSHEV, J. C. ROSSI, G. M. GUSEV and P. BASMAJI, *J. Cryst. Growth* **132** (1993) 533.
13. Y. NOMURA, Y. MORISHITA, S. GOTO and Y. KATAYAMA, *J. Electron. Mater*. **23** (1994) 97.
14. K. HIMURA, M. YAZAWA, T. KATSUYAMA, K. OGAWA, K. HARAGUCHI, M. KOGUCHI and H. KAKIBAYASHI, *J. Appl. Phys*. **77** (1995) 447.
15. JU. R. RO, S. B. KIM, K. W. PARK, E. H. LEE and J. LEE, *J. Cryst. Growth* **202** (1999) 1198.
16. F. NAKAJIMA, J. MOTOHISA and T. FUKUI, *Appl. Surf. Sci*. **162** (2000) 650.
17. J. HIROSE, I. SUEMUNE, A. UETA, H. MACHIDA and N. SHIMOYAMA, *J. Cryst. Growth* **214** (2000) 524.
18. Home built amplification system using a Coherent, Mira 900 oscillator.
19. The wafer was bought from American Xtal Technology, doped with Zn at a concentration $\sim 10^{19}/cm^3$.
20. P. MARKIEWICZ and M. C. GOH, *Langmuirs* **10** (1994) 5.
21. L. N. DINH, KYLE. D. FRISCHKNECHT, M. A. SCHILDBACH, T. ANKLAM and W. MCLEAN II, *J. Vac. Sci. Technol*. A **17** (1999) 3397.
22. L. N. DINH, M. A. SCHILDBACH, M. BALOOCH and W. MCLEAN II, *J. Appl. Phys*. **86** (1999) 1149.
23. D. A. ALLWOOD, R. T. CARLINE, N. J. MASON, C. PICKERING, B. K. TANNER and P. J. WALKER, *Thin Solid Films* **364** (2000) 33.
24. M. YAMADA and Y. IDE, *Jpn. J. Appl. Phys*. **33** (1994) L-671.
25. T. VAN BUUREN, M. K. WEILMEIER, I. ATHWAL, K. M. COLBOW, J. A. MCKENZIE, T. TIEDJE, P. C. WONG and K. A. R. MITCHEL, *Appl. Phys. Letts* **59** (1991) 464.
26. GM32 series from Intelite, Inc.
27. L. N. DINH, L. L. CHASE, M. BALOOCH, F. WOOTEN and W. J. SIEKHAUS, *Phys. Rev*. B **54** (1996) 5029.
28. C. J. SANDROFF, R. N. NOTTENBURG, J.-C. BISCHOFF and R. BHAT, *Appl. Phys. Lett*. **51** (1987) 33.
29. C. J. SANDROFF, J. P. HARBISON, R. RAMESH, M. J. ANDREJCO, M. S. HEGDE, D. M. HWANG, C. C. CHANG and E. M. VOGEL, *Science* **245** (1989) 391.
30. A. J. NOZIK, H. UCHIDA, P. V. KAMAT and C. CURTIS, *Israel J. Chem*. **33** (1993) 15.
31. M. V. RAMAKRISHNA and R. A. FRIESNER, *ibid*. **33** (1993) 3.

Received 18 June 2001
and accepted 14 May 2002